Influence of aggregate mineralogical composition on water resistance of aggregate–bitumen adhesion

Jizhe Zhang, Alex K. Apeagyei *, Gordon D. Airey, James R.A. Grenfell

Nottingham Transportation Engineering Centre, Department of Civil Engineering, University of Nottingham, University Park, Nottingham NG7 2RD, United Kingdom

ARTICLE INFO

ABSTRACT

The effects of aggregate mineralogical composition on moisture sensitivity of aggregate–bitumen bonds were investigated using four aggregate types (two limestone and two granite) and two bitumen grades (40/60 pen and 70/100 pen). Moisture sensitivity (or water resistance) of the aggregate–bitumen bonds were characterized using retained strength obtained from three different tensile tests (peel, PATTI and pull-off). The results showed significant differences in the amount of moisture absorbed by a given aggregate which suggested strong correlations between aggregate mineral composition and moisture absorption. For most of the aggregate–bitumen bonds, failure surfaces transformed from cohesive to adhesive with conditioning time thereby confirming the strong influence of moisture on aggregate bonds. The three tensile tests used in this study showed similar rankings in terms of moisture sensitivity but the pull-off test was found to be the most sensitive. The effect of bitumen on moisture sensitivity was found to be lower than the effect of aggregates, with the moisture absorption properties of the aggregates depending strongly on certain key minerals including clay, anorthite and calcite. Strong correlations were also found between mineral compositions and moisture sensitivity with clay and anorthite having strong negative influence while calcite showed positive effect on moisture sensitivity. Previous studies have identified various mineral phases like albite, quartz, and k-feldspar, as detrimental in terms of moisture sensitivity. The results appear to support the extension of the existing list of detrimental aggregate minerals to include anorthite and clay while supporting the case of calcite as a moisture resistant mineral.

1. Introduction

Asphalt mixtures are widely used as pavement construction materials. During their service life, asphalt pavements have to sustain harsh traffic loads and environmental conditions and deteriorate with the passage of time. One of the major causes of distress in asphalt pavements can be considered to be moisture damage with about 2.8 billion pounds being spent every year on road maintenance across England and Wales [1]. Moisture damage is an extremely complicated mode of asphalt mixture distress that leads to the loss of stiffness and structure strength of the asphalt pavement layers of a road and eventually the costly failure of the road structure [2]. It has been nearly a century since this distress was first recognised [3] although not all damage is caused directly by moisture, its presence increases the extent and severity of already existing distresses like cracking, potholes and rutting [4].

Existence of moisture in the pavement can result in the loss of cohesion within the bituminous binder itself or the loss of interfacial adhesion between binder and the aggregates [5,6]. The resistance of asphalt mixtures to moisture attack has been related to aggregate mineralogy, surface texture of aggregate, bitumen chemistry and the compatibility between bitumen and aggregate [7,8]. In addition, factors such as permeability of the asphalt mixtures, volumetric properties of binder and the ambient conditions are all important when considering the susceptibility of asphalt mixture [9].

With the view to better understand the performance of the aggregate–bitumen interface when exposed to moisture, this paper presents a combination of three different mechanical tests to quantify the damage that occurs at the aggregate–bitumen interface. The focus of this study was limited to the examination of the aggregate–bitumen tensile strength and fracture energy before and after moisture conditioning in the laboratory. The Pneumatic Adhesion Tensile Testing Instrument (PATTI) Test and pull-off Test were conducted to measure the tensile strength of different

* Corresponding author. Tel.: +44 1158468442.
  E-mail address: alex.apeagyei@nottingham.ac.uk (A.K. Apeagyei).

aggregate–bitumen combinations before and after moisture conditioning. Furthermore, the peel test was applied to quantify the fracture energy of different specimens. The retained tensile strength and fracture energy calculated by dividing the values after moisture conditioning by the values before conditioning were used to characterize the moisture sensitivity. Finally, the correlations between these three mechanical tests were presented.

2. Materials

2.1. Bitumen

Two bituminous binders (B1 and B2) with penetration grades of 40/60 pen and 70/100 pen were selected. The physical properties of the bitumen were characterized using softening point (BS EN 1427) and penetration (BS EN 1426) tests. Based on the tests, the softening points of B1 and B2 were 51.2 °C and 45.2 °C respectively, while the measured penetration of B1 at 25 °C was 46 (0.1 mm) compared with 81 (0.1 mm) for B2.

2.2. Aggregates

Four types of aggregate from different quarries were selected as substrates. They included two limestone aggregates (L1 and L2) and two granite aggregates (G1 and G2). These aggregates are known to behave differently in terms of their mineralogical composition and moisture sensitivity.

3. Experimental procedures

3.1. Mineral Liberation Analyser (MLA) test

The mineralogical compositions of aggregates are believed to have a profound influence on moisture damage susceptibility of asphalt mixtures. The mineralogy of the different aggregates was studied using a Mineral Liberation Analyser (MLA) in order to understand the effect of their morphology on moisture damage resistance of aggregate–bitumen bonds. The experimental procedures used for the MLA included the following. Aggregates were first washed in deionised water and then dried in an oven at 40 °C for 24 h. The oven-dried aggregates were then cast in resin moulds with 25 mm diameter and 20 mm height, followed by polishing of the surface using a rotary polishing machine. Finally, carbon coating was applied to form an electrically conductive surface. An FEI Quanta 600 Scanning Electron Microscopy (SEM) with MLA capability was used for the mineral analysis. During testing, the SEM collects back-scattered electron (BSE) images and energy dispersive X-ray data for a series of frames step by step across the specimen surface. Measurement of the backscattered electron

intensities allows for the segmentation of mineral phases within each particle section, while energy dispersive X-ray (EDX) analysis of a given phase allows for phase identification [10]. For each aggregate type, one replicate sample was tested.

3.2. Aggregates moisture absorption

Another important parameter that influences moisture-induced damage in asphalt mixtures is the rate and amount of water absorption of the aggregates. This approach of considering the moisture absorption properties of the aggregate is in contrast to most previous studies that only consider conditioning time when evaluating moisture damage. The current approach recognises the differences in moisture absorption characteristics of different aggregates. To perform the moisture absorption experiments, rectangular aggregate beams with dimensions of 100 mm × 20 mm × 10 mm were first cut from boulders. Then the aggregate beams were cleaned using deionised water and dried in an oven at 40 °C for 24 h to remove all the moisture. The weight of each beam in the dry condition was measured using a balance with the precision of 0.1 μg. All aggregates were moisture conditioned by placing them in baths containing deionised water at 20 °C and weighing them periodically until steady stable conditions were reached. The results from three replicate specimens were used to calculate the mass uptake of aggregates as a percentage of the dry aggregate weight (Eq. (1))

$$\text{Mass uptake } (\%) = M_t = \frac{w_t - w_0}{w_0} * 100 \tag{1}$$

where M_t is the moisture uptake at time t, w_0 is the initial mass of the aggregate in dry condition, w_t is the mass of aggregate after time t.

3.3. Peel test

The peel test (as described in ASTM D6862-11) is used to characterize the adhesive bonds and is widely used in aerospace, automotive and electronics applications [11–13]. Horgnies et al. undertook a peel test to peel bitumen from aggregate surface by using polyethylene terephthalate (PET) as a membrane [14]. Blackman et al. undertook a similar peel test but used an aluminum peel arm rather than a PET membrane [15]. The test is considered to be a reliable method to measure the peel strength (fracture energy) if suitable corrections for plastic work could be performed.

The set-up for the peel test used in this study is shown in Fig. 1. The aggregate substrates with dimensions of 200 mm × 20 mm × 10 mm were prepared as previously described. They were then bonded to aluminum (Alu 1050A) peel arm using bitumen as the adhesive layer. The thickness of the bitumen adhesive layer was controlled by placing five wire spacers on the
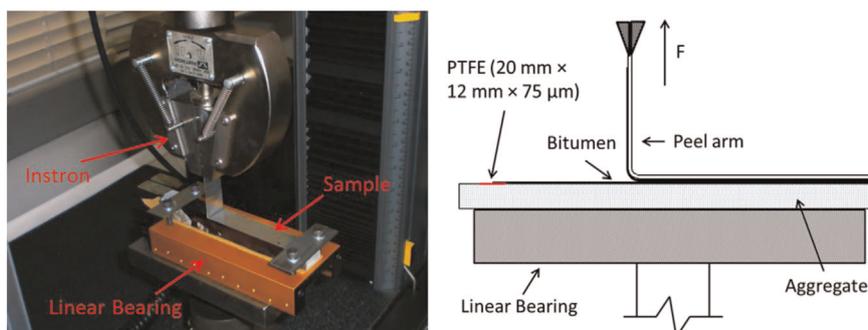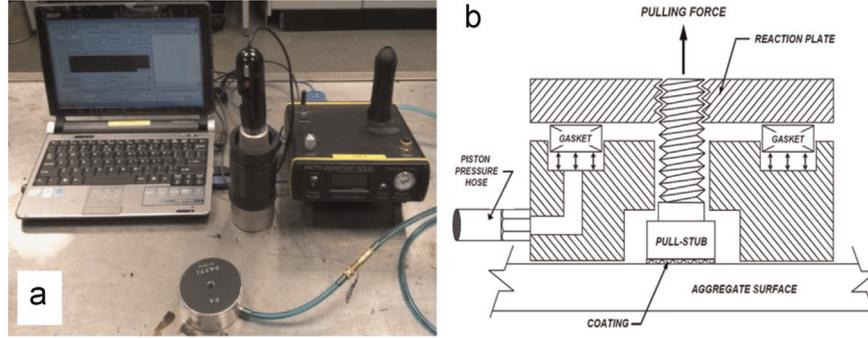

Fig. 1. Details of peel test equipment.

Fig. 2. PATTI test: (a) set-up (b) cross-section view of piston attached to pull-stub [17].

aggregate to produce a 0.25 mm film thickness. The sample pre-paration consists of the following steps [16]:

1. Surface pre-treatment. Aggregate surface and peel arm are wiped gently using a damp paper towel to remove any dust.
2. Pre-heating the aggregate and the bitumen. The aggregate and peel arm are then placed in an oven at 150 °C for 1 h. Bitumen is preheated to 150 °C prior to making the joint.
3. Placing the sharp crack initiator. A release film (PTFE) of dimensions 20 mm × 12 mm × 75 μm is placed on the aggregate surface at one end.
4. Five wire spacers with a length of 20 mm are placed on the aggregate. The diameter of the wire controls the thickness of the bitumen (adhesive) layer.
5. The liquid bitumen is applied (at 150 °C) evenly along the surface of the aggregate.
6. The preheated aluminium peel arm (of length 50 mm longer than the aggregate and of thickness 0.2 mm) is placed on the top of the bitumen layer.
7. Gentle pressure is applied on top of the joint to control the thickness of the bitumen layer. The pressure is uniformly distributed over the bond area. The bonded specimen is then cooled at ambient temperature overnight. The excess adhesive at the edges of the specimen is trimmed with a heated knife.

A universal testing machine which can supply a constant rate of grip separation was used to measure the tensile force during the peel test. The sample was attached to a linear bearing to get a highly accurate and smooth motion during test. During the test, the free end of the peel arm was bent to an applied peel angle of 90° and this angle is maintained by the linear bearing system (Fig. 1). A peel speed of 10 mm/min was used in this test. The tensile force was recorded during the fracture development and the results used to calculate the fracture energy after the plastic work corrections due to the aluminum peel arm had been carried out.

A tensile stress–strain test of the peel arm was performed at a speed of 10 mm/min until fracture occurred. In order to describe the elastic and plastic deformation of the peel arm, the stress–strain curve is fitted according to a bi-linear or power law form [15]. The purpose of the bi-linear and power law curve fits is to get a number of parameters which are used to calculate the fracture energy. The following parameters for the bi-linear model (Eq. (2)) for the peel arm used in this study were used for the plastic deformation corrections as described [15]

$$\sigma = \sigma_y + \alpha E_1(\varepsilon - \varepsilon_y) \tag{2}$$

where $\sigma_y = 26.4$ MPa (yield stress) and $\varepsilon_y = 0.046\%$ (yield strain), $E_1 = 58.2$ GPa (elastic modulus of the peel arm), $\alpha = 0.0215$ ratio of plastic modulus to elastic modulus, $\frac{E_2}{E_1}$.

The corrected adhesive fracture energy G_a could be derived from an energy-balance argument as the difference between the uncorrected adhesive fracture energy G and the energy associated with plastic bending of the peel arm (G_p)

$$G_a = \frac{1}{b}\left(\frac{dU_{ext}}{da} - \frac{dU_s}{da} - \frac{dU_{dt}}{da} - \frac{dU_{db}}{da}\right) = G - G_p \tag{3}$$

where dU_{ext} is the external work, dU_s is the stored strain energy in the peeling arm, dU_{dt} is the energy dissipated during tensile deformation of the peeling arm, and dU_{db} is the energy dissipated during bending of the peeling arm near the peel front.

3.4. Pneumatic Adhesion Tensile Testing Instrument (PATTI) test

The PATTI equipment was used to evaluate the fracture strength of the bitumen–aggregate sample geometry either in terms of the cohesive bond strength of the bitumen or the adhesive bond strength of the bitumen–aggregate interface. This equipment was developed by the National Institute of Standards and Technology (NIST) with the equipment used for the PATTI test shown in Fig. 2a. The PATTI device is used to measure tensile strength, while the camera is used for the analysis of the failure surface. Fig. 2b shows a cross-sectional schematic of the setup of the PATTI with the piston attached to a pull-stub which in turn is attached by means of the bitumen coating to the aggregate substrate [17].

In order to get a well bonded specimen, the aggregate surface and the pull-stub should be wiped carefully using a damp paper towel to remove any dust. After that, the aggregate and pull-stub are placed in an oven and heated to a temperature of 70 °C for one hour. The bitumen must be heated to 150 °C for 1 h to allow it to be fluid enough to coat the aggregate plate. The liquid bitumen is then poured onto a prepared aggregate plate (with the dimension of 100 mm × 100 mm × 20 mm) which is pressed immediately by a metal pull-stub to establish a good bitumen–aggregate bond. In this process the film thickness of bitumen was controlled by the pull-stub itself to make sure all specimens have a 0.8 mm bitumen film, as shown in Fig. 3. Finally, the excess bitumen at the edge of pull-stub should be removed by using a heated palette knife.

During testing, air pressure generated by the PATTI is transmitted to the piston which is placed over the pull stub and screwed onto the reaction plate. The air pressure induces an airtight seal formed between the piston gasket and the aggregate surface. A constant rate of pulling pressure, which is set in the pressure control panel, is applied to the sample. The test generates data in the form of tensile pressure versus testing time which is recorded by the data acquisition system. The maximum tensile pressure to separate the bitumen from the substrate is captured by the software. This pressure is converted to its pull-off tensile strength, as expressed using Eq. (4)

$$POTS = \frac{(BP \times A_g) - C}{A_{ps}} \qquad (4)$$

where, POTS is the pull-off tensile strength (kPa), BP is air pressure (kPa), A_g is the contact area of gasket with relation plate (mm^2), C is the piston constant and A_{ps} is the area of pull-stub (mm^2).

3.5. Pull-off test

The pull-off test used in this study followed the same general principle of the PATTI test in terms of the application of a tensile stress to a thin layer of bitumen sandwiched between two aggregate plates. The pull-off test set-up has been successfully used in the past to evaluate bitumen–aggregate and mastic–aggregate bonds [18]. The innovation of this particular test is the
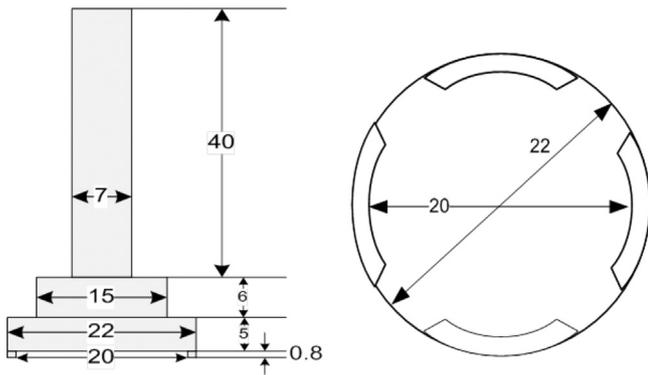

Fig. 3. Pull-stub in profile and bottom views. Note: dimensions are in mm.

ability to accurately determine bitumen film thickness using a modified dynamic shear rheometer (DRS), small aggregate substrate sizes that permit realistic moisture conditioning and simplified custom-made direct tension fixtures that can be easily mounted on a universal testing machine.

Fig. 4 shows the whole procedure in terms of sample preparation and operation of the pull-off test. For sample preparation, boulders of each aggregate were first drilled using a coring tool to get aggregate cylinders with 25 mm diameter. A trimming saw was used to cut the aggregate cylinders into discs with 5 mm thickness. To obtain a relatively constant surface roughness, both surfaces of the aggregate discs were polished using a rotary polishing machine. All discs were cleaned in an ultrasound cleaning machine for 15 min and dried in an oven at a temperature of 40 °C for 24 h. A sample of the finished polished aggregate substrate is shown in Fig. 4A.

A major limitation of some existing pull-off tests and a key motivation for this study is the inability to precisely control bitumen film thickness of test specimens. Two aluminum specimen holding plates (Fig. 4B) were specially designed and fabricated to fit in a standard dynamic shear rheometer (DSR). The plates had dimensions (diameter and thickness) which were similar to a DSR plate. They differ from a DSR top and bottom plate in terms of the provision of sample holders (2 mm tall rings with 3 screen pins, Fig. 4B).

With a view to precisely controlling the film thickness of the bitumen, two modified fixtures were designed to clamp the discs (Fig. 4B) and then fixed into the DSR machine (Fig. 4C). Firstly, the gap between upper and lower surfaces is set to zero and these two surfaces should be parallel. After establishing the zero gap and ensuring that the discs are parallel, a small amount of hot bitumen was placed on the lower aggregate surface (Fig. 4D) and then pressed with the upper aggregate to achieve the required bitumen
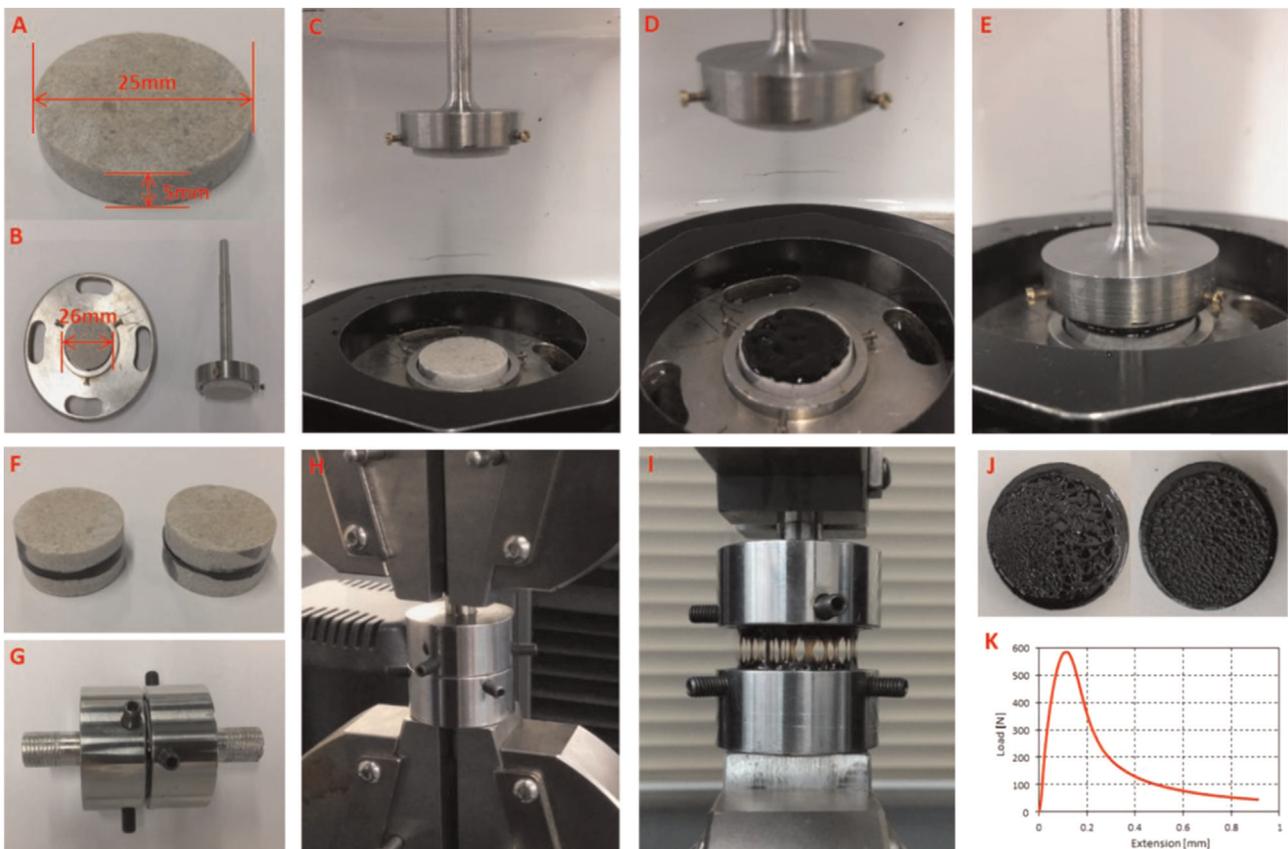

Fig. 4. Pull-off test : sample preparations and test procedures.

film thickness (Fig. 4E), with a gap resolution of 1 µm. In order to simulate the real bitumen film thickness in asphalt mixtures, the bitumen film thickness was controlled at 20 µm. The sample was removed from the DSR after about 15 min of cooling and then the excess bitumen removed by means of a heated palette knife, as shown in Fig. 4F.

Before the pull-off test, the prepared sample was first fixed by two direct tension fixtures with three screws on each, as shown in Fig. 4G. These two fixtures were then installed on a universal testing machine (Fig. 4H). During the test, an extension speed of 10 mm/min and a temperature of 20 °C were applied to break the interface (Fig. 4I). After testing, the failure surfaces of each sample were photographed with a camera (Fig. 4J) and the pull force was recorded by the universal testing machine (Fig. 4K). At least four repeat tests were made for each aggregate–bitumen combination. The results were used to calculate the tensile strength. Tensile strength was computed as the ratio of the peak load divided by the cross-sectional area of the bitumen film, as shown in Eq. (5)

$$TS = \frac{F}{\pi r^2} \tag{5}$$

where TS is tensile strength (kPa), F is the peak tensile force (N) and r is the radius of aggregate disc (m).

3.6. Moisture conditioning

Samples for peel test, PATTI test and pull-off test were subjected the same moisture conditions so as to characterize the relationship between these three methods. To simulate the effect of moisture on the adhesion properties between bitumen and aggregate, the whole specimens were submersed in water at 20 °C for 7 days and 14 days. During the moisture conditioning, moisture could reach the aggregate–bitumen interface in three different ways: through the top and bottom aggregate, through the edge of aggregate–bitumen interface and through the bitumen film. After moisture conditioning, specimens were removed from the water bath and then subjected to the three tests within a few hours. This conditioning method was considered to closely simulate the effect of moisture in an asphalt mixture.

4. Results and discussion

4.1. Aggregate mineralogical composition

The MLA scans and the mineral compositions for the four aggregates are presented in Fig. 5. As shown in this figure, minerals in the granite sample exhibit considerable texture and the distribution is more complex, while the limestone surface is simple and calcite makes up almost all of the area. For the limestone (L1 and L2) samples, calcite is the predominant phase when compared to the other minerals present, with 96.98% and 99.48% by weight, respectively. However, granite is made up of a number of different mineral phases. Chlorite and albite are the dominant minerals in G1 with a presence of 31.53% and 27.13% by weight. In contrast to G1, albite and anorthite are the predominant content minerals in G2, which account for 32.73% and 18.54% by weight, but quartz and chlorite also have significant quantities. The most obvious difference between G1 and G2 is the anorthite content with nearly 19% in G2 and only 0.1% in G1. It is believed that the
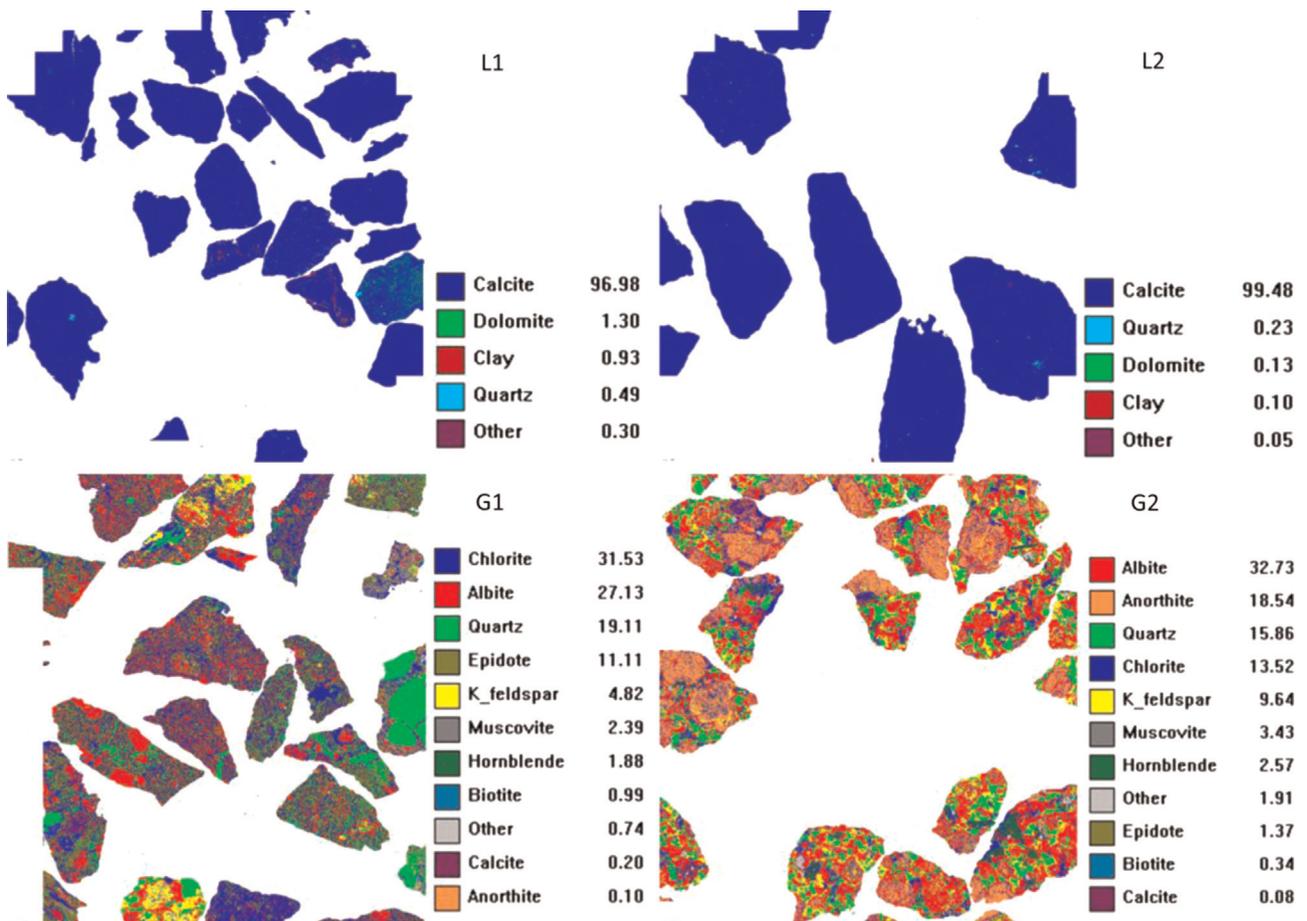

Fig. 5. Mineral mosaic of four aggregates L1, L2, G1 and G2. L1 and L2 are classified as limestone while G1 and G2 are granite.

large proportion of the albite and quartz phases have the potential to lead to moisture damage, due to the poor adhesion between quartz and bitumen. Though albite can form a strong bond with bitumen in dry condition, this bond is quickly broken in the presence of water. There is also evidence that feldspar is responsible for interfacial failure between bitumen and aggregate surfaces [18,19].

4.2. Aggregate moisture absorption

The presence and amount of moisture present at the aggregate–bitumen interface reduces the structural strength due to the loss of the adhesive bond between the bitumen and the aggregate, and/or the loss of the cohesive bond within the bitumen film. Therefore, it is of importance to quantify the absorption properties
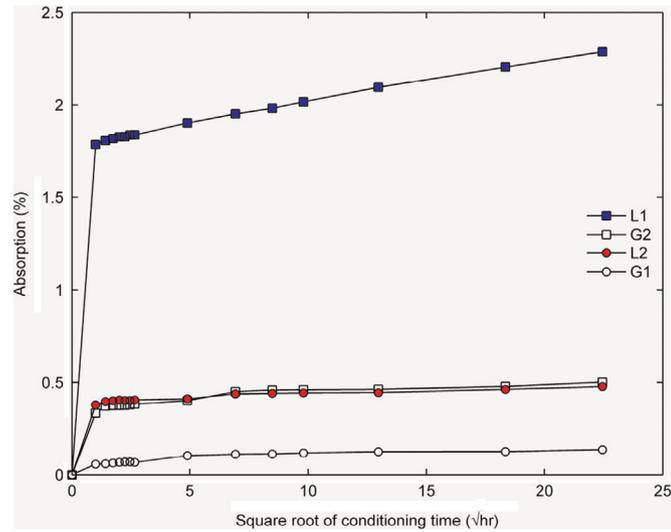

Fig. 6. Moisture absorption versus conditioning time for four different aggregates L1, L2, G1 and G2. Moisture conditioning testing was conducted at 20 °C.

Table 1
Dry fracture energy (J/m²) of aggregate–bitumen bonds at 20 °C. (Peel test).

Sample ID	L1		G1		L2		G2	
	Mean	Std	Mean	Std	Mean	Std	Mean	Std
B1	988	29.7	1015	6.4	981	29.4	1012	16.5
B2	480	13.1	494	19.1	490	13.6	478	21.4

B1=40/60 pen bitumen; B2=70/100 pen bitumen; L1=limestone; G1=granite 1; L2=limestone; G2=granite 2; Std=standard deviation. Note: fracture energy data shown have been corrected for plastic deformation using the energy associated with plastic deformation of the aluminium peel arm, G_p. Average value of G_p was 511 J/m² for B1 and 331 J/m² for B2.

of the aggregates. Many previous studies (e.g. [15–17]) have focused on conditioning time, which even though important, might give misleading results when aggregates of different moisture absorption characteristics are compared. Therefore, in this study, the amount of moisture absorbed as well as the conditioning time was monitored by aggregate specimens measuring 100 mm × 20 mm × 10 mm when submersed in water at 20 °C for up to 21 days. The amount of moisture absorbed was estimated as the percent of the dry weight of the aggregate specimen.

The results are depicted in Fig. 6. The results show that the total amount of moisture absorbed ranged from about 0.13% for aggregate G1 to about 2.25% for aggregate L1. The results suggest the rather large differences in water absorption could be due to the different mineralogy and structure of the aggregates. A regression analysis was performed to develop a statistical model by relating the aggregate mineralogical data presented in Fig. 5 with the aggregate moisture absorption (equilibrium moisture) depicted in Fig. 6. The results of regression analysis identified three mineral components – calcite, clay and anorthite – as the most significant factors that influence aggregate moisture absorption. The model (Eq. (6)) showed excellent correlation ($R^2 = 0.999$). As shown in Eq. (6), of the three factors, clay appears to be the most significant factor. The results agree with common knowledge [AASHTO T 176 and ASTM D2419]

$$M = 0.097455 + 2.1142*clay + 0.02175*anorthite$$
$$+ 0.001921*calcite \qquad (6)$$

where M is the equilibrium moisture absorption; clay is the amount of clay minerals (%); dolomite is the amount of anorthite (%) and calcite is the amount of calcite (%).

The results show the moisture absorption properties of mineral aggregates depend strongly on certain key mineral content especially the clay content, for the aggregates considered in this study.

4.3. Peel test – fracture energy of aggregate–bitumen bonds

The purpose of the peel test was to determine the fracture energy of the aggregate–bitumen bonds as a function of aggregate type and moisture conditioning time. Results are presented for four replicate tests performed on each aggregate–bitumen combination. The average force of each sample, the peel angle, the specimen width, (not shown here for lack of space) and the parameters in Eq. (2) describing the plastic deformation in the peel arm were entered into the Microsoft excel macro IC Peel software to the calculate fracture energy [20]. The average values obtained for the energy associated with plastic deformation in the peel arm (G_p) were 511 J/m² and 331 J/m², respectively for 40/60 pen bitumen and 70/100 pen bitumen. The values compare very well with the G_p of 505 J/m² reported in [15] for a 40/60 pen bitumen. Table 1 shows the average fracture energy and test variability (standard deviation) of all specimens before moisture
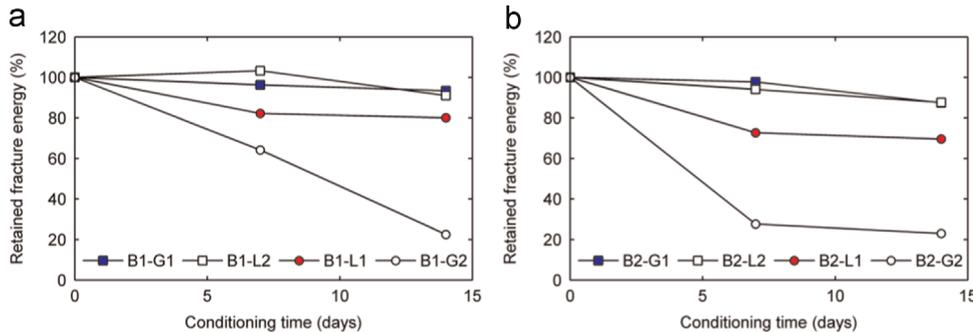

Fig. 7. Effect of moisture conditioning time on retained fracture energy of different aggregate–bitumen combinations. (a) Bitumen B1 and (b) bitumen B2.

condition. The standard deviation suggests that the peel test has low variability (COV 4.48%) which compares quite well with the variability of ±9% reported in [15]. From Table 1, it can be seen that specimens prepared with the same bitumen have almost the same fracture energy in the dry condition, irrespective of which aggregate was used. The results suggest that in the dry state, cohesive failure controls the aggregate–bitumen bond and that failure location is within the bitumen. These assertions agree with previous studies [15–18] related to dry aggregate–bitumen bonds. However, specimens prepared with B2 bitumen have significantly lower fracture energy than those with B1 bitumen. This is because B1 is stiffer than B2, so higher energies needed to break it apart. This indicates that bitumen properties control the fracture energy in the dry condition.

In order to analyse the influence of bitumen on moisture damage for the same aggregate, the retained fracture energy of specimens after 7 days and 14 days moisture conditioning were calculated by dividing the conditioned fracture energy by the dry fracture energy, and the results are shown in Fig. 7. After moisture conditioning, most of the specimens experienced a decrease in fracture energy, except for B1–L2 after 7 days condition. However, the specimens showed different fracture energy losses due to their different aggregate–bitumen combinations. For example, fracture energy losses in the samples containing G1 and L2 were the lowest for both bitumen types. The specimens prepared by G2 showed the highest fracture energy losses after moisture conditioning. It can be seen that, for the four aggregates used in this research, specimens containing the B1 bitumen showed higher percent retained fracture energy than those containing B2 bitumen. So, it can be concluded that changing the binder grade from 40/60 pen to 70/100 pen produced a decrease in moisture durability for most aggregates, based on the peel test. However, based on the results shown in Fig. 7, it appears that the effect of bitumen on moisture sensitivity of aggregate–bitumen mixtures is minimal compared to the aggregate effects.

The results presented in Fig. 7 show that the G1 and L2 aggregates have the highest retained fracture energy, with around 90% retained fracture energy after 14 days moisture conditioning.

L1 aggregate has the medium retained fracture energy, with about 80% retained fracture energy for B1 bitumen compare with 70% for B2 bitumen. The lowest result belongs to G2 aggregate, with only 23% of fracture energy retained after moisture conditioning for both types of bitumen.

The differences in moisture durability could be attributed to the mineral composition and water absorption of aggregates. As previously discussed, there is a strong correlation ($R^2 = 0.999$) between certain aggregate minerals and aggregate moisture absorption. On this basis alone, it should be expected that degradation of bond strength in the presence of moisture should also be correlated to aggregate mineralogy. In an attempt to establish such relationship, regression analysis using the retained fracture strength data presented in Fig. 7 and the mineralogical data presented in Fig. 5 were conducted resulting in the model shown in Eq. (7). The model showed excellent correlation ($R^2 = 0.999$) similar to the results obtained for moisture absorption (Eq. (6)). The results support the assertion that moisture sensitivity of aggregate–bitumen bonds are influenced mainly by the aggregate mineralogy. The model in Eq. (7) also shows the detrimental effects of certain minerals such as clay and anorthite on moisture susceptibility. The signs of the model parameters in Eq. (7) are revealing. For example, calcite carries a positive sign suggesting positive correlation between amounts of calcite moisture and resistance. The results agree with general experience [2,4–7,18]. Clay and anorthite carry negative signs, this suggests these minerals are negatively correlated with moisture resistance and thus have detrimental effects on moisture damage resistance of asphalt mixtures. Previous studies like Horgnies et al. have identified albite, quartz, and k-feldspar as minerals with detrimental effect on aggregate–bitumen bond [18]. The results of the current study provide evidence for extending the list of detrimental aggregate minerals to include clay and anorthite as well as supporting the case of considering calcite as moisture resistant mineral

$$RS = 91.363623 + 0.3211*calcite - 15.5659*clay$$
$$- 3.68743*anorthite \tag{7}$$

where RS is retained strength; calcite is amount of calcite (%); clay is amount of clay minerals (%) and anorthite is amount of anorthite (%).

4.4. PATTI test

For each aggregate–bitumen combination, four specimens were tested to get their average result to compare with other conditions. Through this test, the tensile strength can be measured and an image of the failure surface taken. The average tensile strength results before moisture conditioning are shown in Table 2. In the
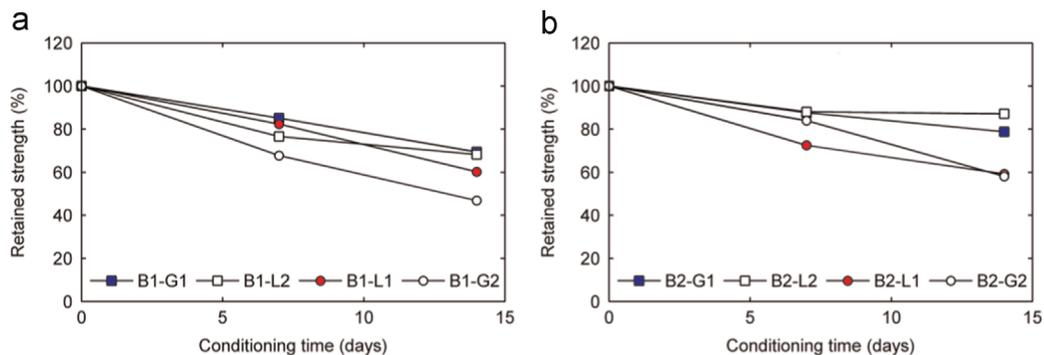
Table 2
Dry tensile strength (kPa) of aggregate–bitumen bonds at 20 °C (PATTI).

Sample ID	L1		G1		L2		G2	
	Mean	Std	Mean	Std	Mean	Std	Mean	Std
B1	1820	70.8	1831	184.9	1805	209	1840	137.6
B2	1359	97	1504	104	1495	44.5	1486	117.4

B1=40/60 pen bitumen; B2=70/100 pen bitumen; L1=limestone; G1=granite 1; L2=limestone; G2=granite 2; Std=standard deviation.

Fig. 8. Retained bonding strength obtained from the PATTI test after moisture conditioning showing the effect of aggregate type on moisture sensitivity of aggregate–bitumen bonds at 20 °C.

dry condition, specimens prepared with B1 bitumen showed higher tensile strength than those prepared with B2 bitumen. In addition, the aggregate type did not influence the tensile strength when used with the same bitumen. The phenomenon in dry condition correlates well with the peel test results.

The differences in moisture sensitivity for different aggregate–bitumen combinations could be explained by the remaining percentage of bond strength after moisture conditioning which was achieved by dividing the conditioned bonding strength by the dry bonding strength, as shown in Fig. 8. From this figure it is clear that all samples experienced a decline in their retained bonding strength after moisture conditioning. However, the declining rates of bonding strength are different for different bitumen aggregate combinations. In terms of the B1 bitumen, as shown in Fig. 8a, specimens prepared with G1 and L2 aggregates have the highest retained strength with the results being 69% and 68%, respectively, after 14 days of moisture conditioning. This means that G1 and L2 aggregates have good moisture resistance. However, G2 aggregate shows the lowest retained strength which means poor moisture resistance. Specimens prepared with B2 bitumen (Fig. 8b) showed the same ranking, with G1 and L2 aggregates having the best resistance to moisture-induced damage, while G2 aggregate shows the worst moisture resistance. For most aggregates (except L1), specimens prepared with B2 bitumen tend to retained higher tensile strength in comparison with B1 bitumen.

4.5. Pull-off test

All pull-off tests were performed at a temperature of 20 °C with the same extension speed as the peel test (10 mm/min). In order to simulate the real bitumen film thickness in asphalt mixtures, the bitumen film thickness was controlled at 20 μm. During the pull-off test, because the L1 aggregate is very soft, the fixtures could not mount the specimens properly. So, the samples prepared with L1 aggregate tended to break in the aggregate rather than the bitumen film or aggregate–bitumen interface. An alternative method to mount L1 specimens into the fixtures will need to be designed in the future. So, only specimens prepared with G1, L2 and G2 achieved reliable results.

Table 3
Dry tensile strength (kPa) of aggregate–bitumen bonds at 20 °C (pull-off).

Sample ID	G1		L2		G2	
	Mean	Std	Mean	Std	Mean	Std
B1	1947	199	1920	103	1938	312
B2	1386	72	1425	147	1413	128

B1=40/60 pen bitumen; B2=70/100 pen bitumen; G1=granite 1; L2=limestone; G2=granite 2; Std=standard deviation.

Due to their much smaller dimensions, the moisture damage process for the pull-off test is faster than the peel or PATTI tests. The specimen prepared with G2 aggregate separated at the bitumen–aggregate interface without loading after 14 days moisture conditioning thereby its demonstrating that 14 days of conditioning time is too long to get comparable results with the PATTI test. In this part of the study, the conditioning time were shortened to 1 and 7 days.

Four replicate tests were performed on each aggregate–bitumen combination. The average tensile strength of each aggregate–bitumen bond in the dry condition was calculated using Eq. (5). The results are depicted in Table 3 together with the test variability (standard deviation); the latter suggesting the new pull-off test has low variability with a coefficient of variability ranging from about 5–16%. It can be seen from Table 3 that samples prepared with bitumen B1 have higher tensile strength in comparison with bitumen B2. This phenomenon correlates well with the peel and PATTI tests. In terms of the same bitumen, samples prepared with different aggregates tended to yield similar tensile strength. This suggests that, in the dry condition, the tensile strength of samples is controlled mainly by the bitumen properties, aggregate effects appear minimal. One reason for this observation is that damage was mainly cohesive (i.e. within the bitumen) and not interfacial.

Fig. 9 shows the effect of conditioning time on retained tensile strength of the aggregate–bitumen bond. From this figure it can be seen that specimens which contain L2 or G1 aggregate show good moisture resistance with over 75% tensile strength retained after 7 days conditioning. On the contrary, the moisture effect was more pronounced in the specimens containing G2 aggregate where the strength decreased by over 80% and 40% for B1 and B2 bitumen, respectively. Aggregate L2 and G2 have similar moisture absorption properties (as shown in Fig. 6) but they show obviously different moisture sensitivity. This result suggests moisture absorption alone is not an indicator of moisture damage, the mineralogy of the aggregate is also important. Another reason for the differences observed in L2 and G2 could be that because G2 contains a large amount of albite and quartz, the bonds formed with bitumen are quickly broken in the presence of water. The results showing better resistance to moisture-induced damage for specimens containing limestone than granite are in agreement with previous studies [5,18]. However, G1 is granite, but because of its lower moisture absorption, it is hard for water to diffuse through the aggregate into the aggregate–bitumen interface so it cannot weaken the bond. On this basis, it is reasonable to state that the moisture-induced damage of aggregate–bitumen bonds is not only controlled by the mineralogical composition but the moisture absorption of the aggregate should also be considered. The differences in retained strengths between G1 and G2 could be attributed to higher moisture absorption of the latter. This result
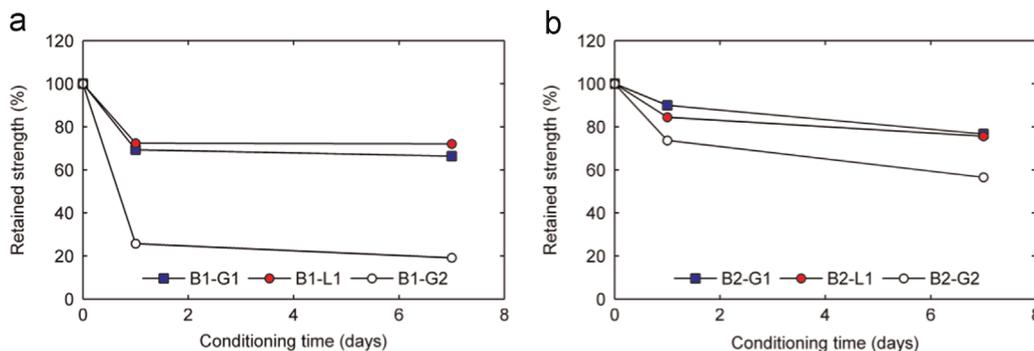

Fig. 9. Effect of moisture conditioning time on tensile strength of different aggregate–bitumen combinations. In general acidic aggregate performed worse than basic aggregates. The combination of bitumen B1 with aggregate G2 performed worst.
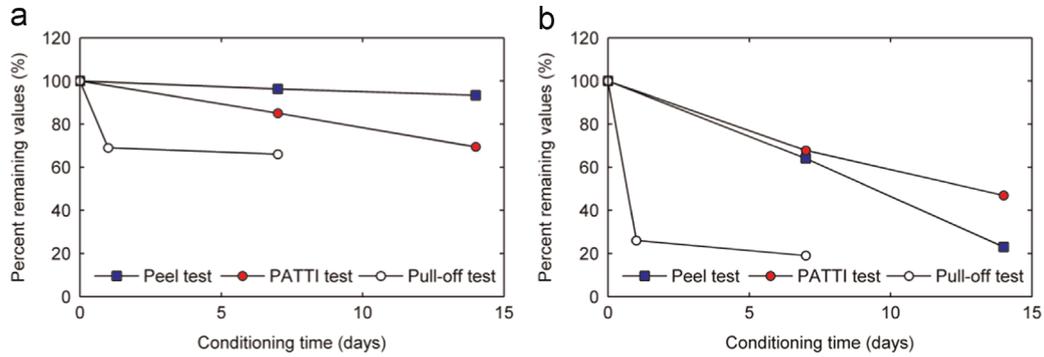
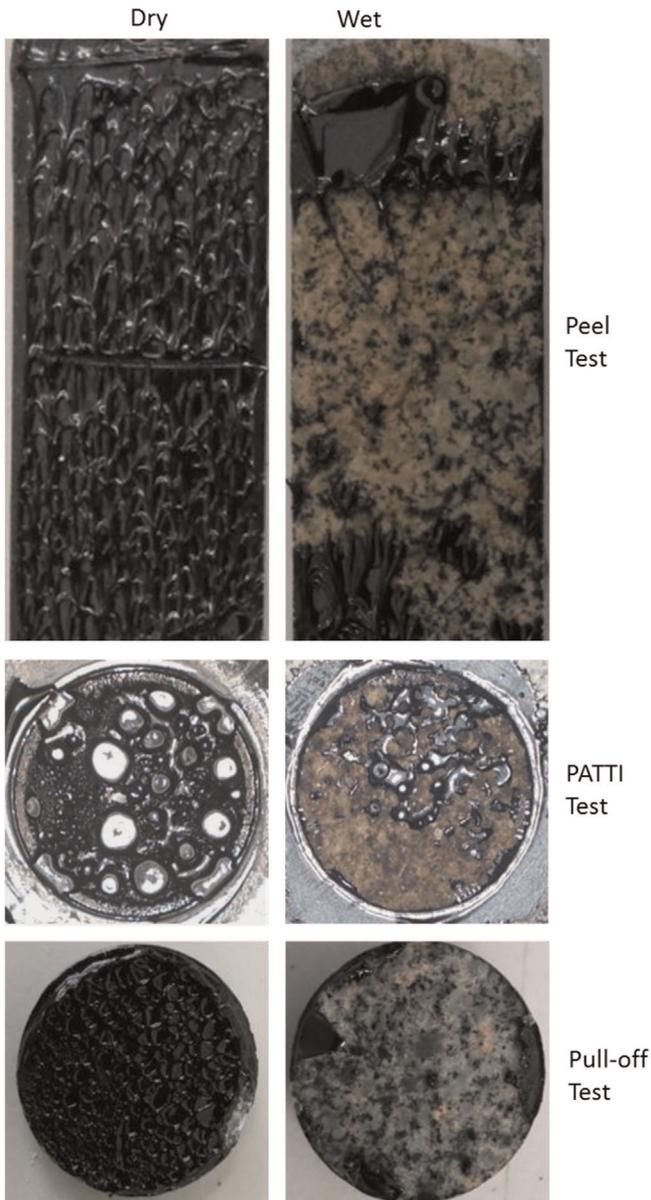**Fig. 10.** Comparison of three mechanical tests for (a) B1–G1 and (b) B1–G2.

Fig. 11. Sample failure surfaces for dry and moisture-conditioned aggregate–bitumen (B1–G2) bonds tested in tension using peel test (upper plate), PATTI test (middle plate) and pull-off test (bottom plate). In all cases, failure mode was cohesive for dry specimens and adhesive for wet specimens. Note: moisture conditioning time for the pull-off test was seven days compared with 14 days for both the peel and PATTI tests.

combined with the L2 results previously discussed leads one to conclude that for susceptible aggregates, the amount of moisture absorption is a significant factor.

In terms of the same aggregate, specimens prepared with B2 bitumen show better resistance to moisture damage in comparison with B1. This demonstrated that softer bitumen with lower complex modulus may have better performance in the presence of moisture. However, more tests need to be done to confirm this conclusion.

4.6. Comparison of three test methods

All the three methods used in this study can be considered as tensile in nature. The major differences are in terms of specimen geometry and loading rate. A key objective of this study was to determine the moisture sensitivity of aggregate–bitumen combinations by three different mechanical tests as a function of aggregate mineralogy. Another objective was to determine which of these three tests was most sensitive to experimental variables – aggregate type, bitumen type and moisture absorption. A test was considered sensitive if it can distinguish between the various aggregates and/or the different bitumen used.

Results with G1 and G2 aggregates were selected for comparison as shown in Fig. 10. From Fig. 10a it can be seen that for the same aggregate–bitumen combination, the peel test retained the highest value while the pull-off test retained the lowest result under the same moisture conditioning. It means that for the peel test more time will be needed to damage the aggregate–bitumen interface. However, the pull-off test will take the least time to make the same moisture damage. For B1–G2 specimen as shown in Fig. 10b, although the peel and PATTI tests show different ranking from B1–G1, the pull-off test still shows the lowest result. So, the pull-off test appears to be the most sensitive test for evaluating moisture sensitivity. This may be because the specimen used for the pull-off test is the smallest and therefore less time is needed to achieve the same level of saturation in the pull-off test compared with the peel and PATTI tests.

The failure surfaces of B1–G2 samples achieved from all three tests before and after moisture conditioning are shown in Fig. 11. Without moisture conditioning, a cohesive failure occurred within the bulk of the bitumen, as shown in Fig. 11 (a1, b1 and c1). The fracture energy depended on the cohesive bond in the bulk bitumen layer. That is why all aggregates show almost the same fracture energy and tensile strength in the dry condition. After moisture conditioning, water penetrated into the specimen and weakened the aggregate–bitumen interface. The failure surfaces tend to transform from cohesive to adhesive, as shown in Fig. 11 (a2, b2 and c2). However, less time was needed for the pull-off test

(7 days) to achieve adhesive failure in comparison with the peel and PATTI tests (14 days). This phenomenon also supports the assertion that the pull-off test is the most sensitive test to measure the moisture sensitivity of aggregate–bitumen combinations.

5. Conclusions and recommendations

The effects of aggregate mineralogical composition on moisture sensitivity of aggregate–bitumen bonds were investigated using four aggregate types (two limestone and two granite), two types of bitumen (40/60 pen and 70/100 pen) and three mechanical tests: peel test, PATTI test and pull-off test, as a function of moisture immersion time. Retained strength was used as measure of moisture sensitivity of aggregate–bitumen bonds. The results were analysed by relating aggregate moisture absorption and mineral composition to retained bond strength. The following conclusions were reached based on the results presented in this paper:

- The results showed significant differences in the amount of moisture absorbed by a given aggregate. For the four aggregates considered, equilibrium moisture absorption varied from 0.1% to 2.25%. The results suggest strong correlations between aggregate mineral composition and moisture absorption.
- For most aggregates, the loci of failure changed from cohesive to adhesive with the conditioning time which supports the strong influence of moisture on bitumen–aggregate bonds.
- The three tensile tests used in this study showed similar ranking in terms of moisture sensitivity but the pull-off test was found to be the most sensitive. The high sensitivity of the pull-off test could be attributed to smaller specimen geometry that allowed faster moisture diffusion into the aggregate–bitumen interface where damage is believed to be initiated.
- The effect of bitumen on moisture sensitivity was lower than the effect of aggregates.
- The results show that, for the aggregates considered in this study, moisture absorption properties of aggregates depend strongly on certain key minerals including clay, anorthite and calcite. Strong correlations were also found between mineral compositions and moisture sensitivity with clay and anorthite having strong negative influence while calcite showed positive effect on moisture sensitivity.
- Previous studies have identified various mineral phases like albite, quartz, and k-feldspar, as detrimental in terms of moisture sensitivity. The current study extended this list of detrimental aggregate minerals to include anorthite and clay while supporting the case of calcite as a moisture resistant mineral.

Acknowledgements

Reference

[1] Annual Local Authority Road Maintenance (ALARM) Survey 2014. Asphalt Industry Alliance, ⟨http://www.asphaltindustryalliance.com/images/library/files/ALARM_Survey_2014.pdf⟩ [accessed 03.07.14].
[2] Airey GD, Collop AC, Zoorob SE, Elliott RC. The influence of aggregate, filler and bitumen on asphalt mixture moisture damage. Constr Build Mater 2008;22 (9):2015–24.
[3] Nicholson V. Adhesion tension in asphalt pavements, its significance and methods applicable in its determination. J Assoc Asph Paving Technol 1932;3:28–38.
[4] Grenfell JRA, Ahmad N, Liu Y, Apeagyei AK, Large D, Airey GD. Assessing asphalt mixture moisture susceptibility through intrinsic adhesion, bitumen stripping and mechanical damage. Road Mater Pavement Des 2014;15(1):131–52.
[5] Airey GD, Choi YK. State of the art report on moistures test methods for bituminous pavement materials. Road Mater Pavement Des 2002;3(4):355–72.
[6] Liu Y, Apeagyei AK, Ahmad N, Grenfell JRA, Airey GD. Examination of moisture sensitivity of aggregate–bitumen bonding strength using loose asphalt mixture and physico-chemical surface energy property tests. Int J Pavement Eng 2014;15(7):657–70.
[7] Terrel RL, Al-Swailmi S. Water Sensitivity of Asphalt–Aggregate Mixes: Test Selection. SHRPA-403, Strategic Highway Research Program. Washington, DC: National Research Counci; 1994.
[8] Abo-Qudais S, Al-Shweily H. Effect of aggregate properties on asphalt mixtures stripping and creep behaviour. Constr Build Mater 2007;21(9):1886–98.
[9] Grenfell J, Ahmad N, Airey GD, Collop AC, Elliott R. Optimising the moisture durability SATS conditioning parameters for universal asphalt mixture application. Int J Pavement Eng 2012;13(5):433–50.
[10] Ahmad N. Asphalt Mixture Moisture Sensitivity Evaluation using Surface Energy Parameters. Nottingham: University of Nottingham; 2011 March.
[11] Kawashita LF, Moore DR, Williams JG. Analysis of peel arm curvature for the determination of fracture toughness in metal-polymer laminates. J Mater Sci 2005;40(17):4541–8.
[12] Horgnies M, Willieme P, Gabet O. Influence of the surface properties of concrete on the adhesion of coating: characterization of the interface by peel test and FT-IR spectroscopy. Prog Org Coat 2011;72(3):360–79.
[13] Leforestier E, Darque-Ceretti E, Peiti D, Bolla M. Peeling and characterisation of the carbon fibre-based radicular adhesive anchorage interface. Int J Adhes Adhes 2007;27(8):629–35.
[14] Horgnies M, Darque-Ceretti E, Fezai H, Felder E. Influence of the interfacial composition on the adhesion between aggregates and bitumen: investigations by EDX, XPS and peel tests. Int J Adhes Adhes 2011;31(5):238–47.
[15] Blackman BRK, Cui S, Kinloch AJ, Taylor AC. The development of a novel test method to assess the durability of asphalt road-pavement materials. Int J Adhes Adhes 2013;42:1–10.
[16] Cui S, Blackman BRK, Kinloch AJ, Taylor AC. Durability of asphalt mixtures: effect of aggregate type and adhesion promoters. Int J Adhes Adhes 2014;54:100–11.
[17] Santagata FA, Cardone F, Canestrari F, Bahia HU. Modified PATTI test for the characterization of adhesion and cohesion properties of asphalt binders. In: International Conference on Maintenance and Rehabilitation of Pavements and Technological Control, Sixth Proceedings. Turin; 2009.
[18] Apeagyei AK, Grenfell JRA, Airey GD. Moisture-induced strength degradation of aggregate–asphalt mastic bonds. Road Mater Pavement Des 2014;15 (1):239–62.
[19] Pasandin AR, Perez I. The influence of the mineral filler on the adhesion between aggregates and bitumen. Int J Adhes Adhes 2015;58:53–8.
[20] IC Peel software, ⟨http://www3.imperical.ac.uk/meadhesion/testprotocols/peel⟩, Imperial College London [accessed 14.03.13].